Rainfall-generated, near-surface turbulence

Jose Beya[1], William Peirson[2], Michael Banner[3]

[1] *Water Research Laboratory, School of Civil and Environmental Engineering, University of New South Wales,110 King St. Manly Vale 2093, NSW, Australia, e-mail: j.beya@wrl.unsw.edu.au*

[2] *Water Research Laboratory, School of Civil and Environmental Engineering, University of New South Wales,110 King St. Manly Vale 2093, NSW, Australia, e-mail: w.peirson@unsw.edu.au*

[3] *School of Mathematics, University of New South Wales, UNSW Kensington, 2052, NSW, Australia, email: m.banner@unsw.edu.au*

Abstract. An investigation of the development of turbulence adjacent to the free surface irradiated with vertical rainfall has been completed. Laboratory measurements of turbulence profiles under simulated rainfall were carried out with a micro acoustic Doppler velocimeter (ADV). Data processing techniques based on spectral analysis were used to extract the low levels of turbulence from the velocity time series. Turbulence profiles showed a rapid decay with depth and weak dependency on rainfall intensity in agreement with Braun (2003). However these observations are inconsistent with the high levels of turbulence dissipation recently reported by Zappa *et al*. (2009). The energy transfer from rainfall to sub-surface turbulence is an inefficient process. Significant rainfall energy is dissipated at the air-water interface where the interaction of capillary ripples, drop splashes, air entrainment and other complex processes take place.
Key Words: turbulence, rainfall, free surface.

1. Introduction

This article originated from a study where the main purpose was to measure wave attenuation caused by surface turbulence. Vertical rainfall was selected as the turbulence generating mechanism for the following reasons:

1) Turbulence diffuses from the surface in a similar manner to whitecapping and wind shear generated turbulence in the ocean (Craig and Banner 1994).
2) No net horizontal momentum is imparted to the propagating waves.
3) It is steady and homogeneous across the surface which simplifies analysis when compared with turbulence generated by wind and breaking waves where turbulence cannot be easily separated from propagating waves and where bursting events are present, inducing a non-stationary process (Kawamura and

Toba, 1988; Rapp and Melville 1990).

4) Past studies have assumed a direct relationship between the rainfall kinetic energy flux (*KEF*) and the turbulence dissipation implying the *KEF* had a direct influence in wave attenuation (Tsimplis 1992, Poon *et al.* 1992, Le Mehaute and Khangaonkar 1990).

The original idea was to measure the attenuation of waves caused by different levels of surface turbulence controlled by varying the intensity of simulated rainfall (i.e. rainfall *KEF*) in order to provide a good data set to validate existing wave-turbulence interaction theories.

However in preliminary observations showed that turbulence was not as strong as originally anticipated. Further, turbulence and wave attenuation were found to be weakly dependent on rainfall intensity. Our findings, although initially unanticipated, are consistent with:

1) Braun (2003) who carried out ADV and PIV turbulence measurements under simulated rainfall and found similar turbulence levels. She tested a wide range of rainfall rates (8, 40 and 216 mm h^{-1}) produced by hypodermic simulators that generated impacting raindrops with less than terminal velocities.

2) Poon *et al.* (1992) and Tsimplis (1992) who reported measurements of wave attenuation due to rainfall. Their observations showed no perceptible differences in the wave attenuation coefficient for the range of rainfall rates tested. They used smaller facilities and rainfall simulators that produced raindrops with impact velocities significantly less than terminal. Both studies recommended the characterization of the turbulence profile simultaneously with the wave attenuation.

3) Bliven *et al.* (1997) who reported a weak variation in the raindrop wave spectra for different rainfall rates. Their measurements involved a broad range of rainfall intensities generated with a hypodermic needle rainfall simulator in which raindrops achieved impact velocities close to terminal. They recommended wave and turbulence measurements to resolve whether a possible “saturation” limit and an interaction between waves and turbulence exists.

Many studies have assumed that the energy transfer from rainfall to subsurface turbulence is a strong process (Houk and Green 1976, Manton 1973, Nystuen 1990, Craeye and Schlüssel 1998) while the evidence we are presenting indicates the contrary. Focus on this issue should be of primary importance for those investigators concerned about the air-water interaction processes under rainfall conditions and radar scatterometer measurements.

In this contribution we first describe the measurement techniques used to obtain the turbulence statistics. Results are then compared with previous studies by Braun (2003) and Zappa *et al.* (2009). Finally an analysis on the rainfall energy budget and a comparison to the Craig and Banner (1994) turbulence diffusion

model results are presented.

2. Test facility

The test facility was a water tank with glass sidewalls of 30m long, 0.6m wide and 0.6m total depth (Figure 1). The mean water depth was maintained at 0.415m ±1mm for all experiments by an automatic control system. Over the measurement period, the water temperature varied from 10.9 to 12°C.

Vertical artificial rain was generated with a simulator physically identical to that developed by Shelton *et al.* (1985) which was designed and shown to produce near uniform droplet fields with size distributions similar to natural rainfall at terminal vertical velocities across a range of rain intensities from 85 to 168 mm h^{-1}. Eight 30WSQ nozzles were installed at 3.00m above the tank surface located with a spacing of 2.13m along the tank. Separate water and air manifold systems supplied pressurised air and water immediately upstream of the nozzles, the compressed air increasing the exit velocity of the water droplets. Water from the tank was recirculated through the rainfall system. The mean flow rate was controlled by a rotameter.

During this investigation, measurements were undertaken for two rainfall conditions: a so-called low rainfall (LR) of 108 ± 7mm h^{-1} and a high rainfall (HR) of 141 ± 6mm h^{-1}. These conditions were achieved by setting the flow rates and nozzle air pressures in accordance with the corresponding values in Table 2 of Shelton *et al.* (1985). Rainfall intensity and uniformity was confirmed during the experiments by visual inspection and measurements using temporary rain gauges located beneath each nozzle.

The tank was equipped at one end with a flexible plate wave generator. The

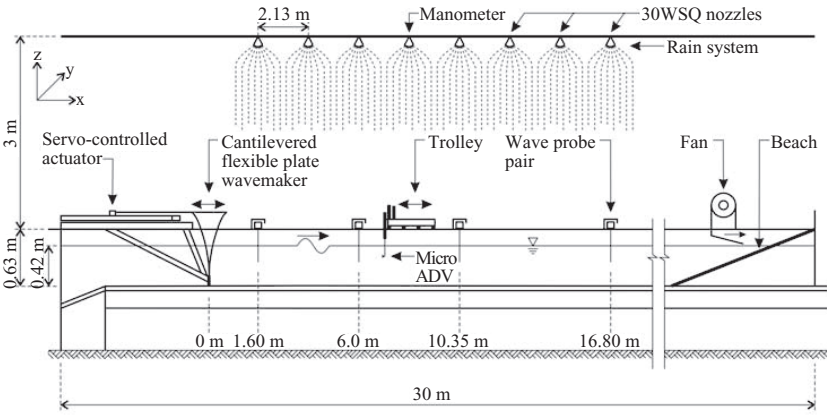

Figure 1 Schematic diagram showing experimental layout and key equipment (not to scale).

other end had a gently-sloping beach where waves were absorbed. Any slicks on the surface of the tank were carefully visually monitored and, prior to testing each day, removed by generating steep waves for approximately 1 hour which carried any surface material to the downstream end of the tank by the Stokes drift. A fan was used to ensure that surface slick material was swept to and retained on the beach (Figure 1).

3. Velocity intensity profiles

The near-surface velocity field generated by the rain was measured in the

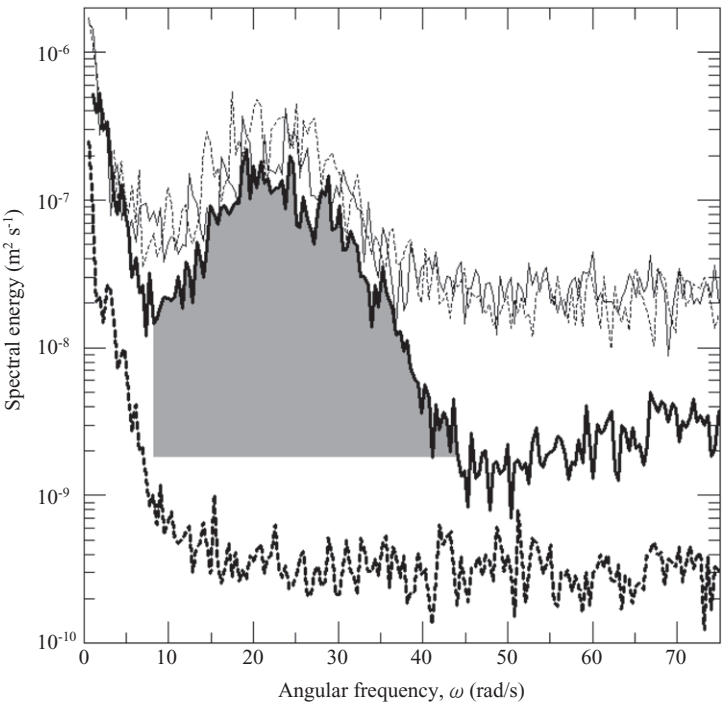

Figure 2 Representative fluctuating velocity spectra under LR obtained from the acoustic Doppler velocimeter in static mode focusing at 31mm depth, *u'* heavy solid line, *v'* light solid line, *w'* light dashed line. Note the clearly defined minimum in spectral energy at approximately 8rad s^{-1} and approximately constant acoustic noise level above 45rad s^{-1}. Note also the much lower acoustic noise of the head-normal velocity component. Spectra in this plot were smoothed with 11 point bin averages. The heavy dashed line shows the *u'* spectrum case NR focusing at 31mm depth. The area in grey indicates the spectral partitioning used for the calculation of *u'*. Similar partitioning was applied to the *v'* and *w'* components.

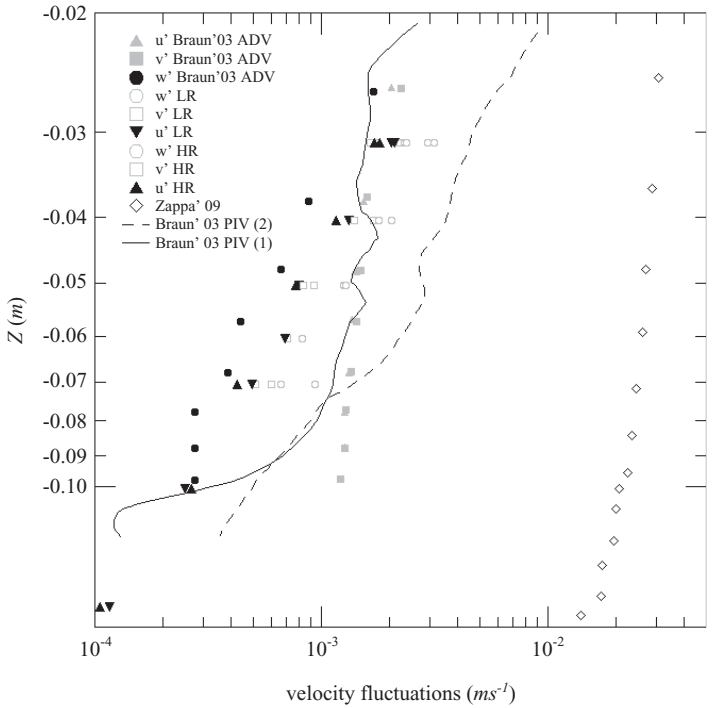

Figure 3 Vertical profiles of velocity fluctuations obtained from the static ADV measurements for both rainfall conditions during this investigation shown in comparison with other studies. *u'* velocity component for LR and HR conditions are indicated by downward and upward pointing triangles respectively. *v'* and *w'* components represented by gray hollow squares and circles respectively (larger symbols HR, smaller LR). Multiple identical symbols indicate repeat measurements. The maximum deducted RMS acoustic noise were 5.1×10^{-4} m s^{-1} for the *u'* component and 2.1×10^{-3} m s^{-1} for the *v'* and *w'* components. Note the close proximity of the velocity components indicating isotropy over the entire profile. The least noisy component from the ADV data of Braun (2003) (40mm h^{-1}), is indicated by black solid circles (*w'*). Grey solid triangles and squares indicate her *u'*, *v'* components respectively. Note the similarity of her *u'*, *v'* measurements that indicates isotropy whilst the *w'* component (with lower acoustic noise) is systematically less than the corresponding *u'*, *v'* values. Braun (2003) particle image velocimetry measurements are shown as solid line (8mm h^{-1}, 2.1mm drop diameter)[1] and dashed line (216mm h^{-1}, 2.9mm drop diameter)[2]. Hollow diamonds are estimated velocity intensities obtained from the turbulent dissipation measurements of Zappa *et al*. (2009) using equations (2) and (3) and the value of z_0 found in this study.

absence of any mechanically-generated waves using a Sontek A827 side-looking 16MHz, 5cm focal distance, three-dimensional micro acoustic Doppler velocimeter (ADV). The ADV was used to measure the vertical profile of the velocity fluctuations near the water surface under rainfall. The ADV was mounted

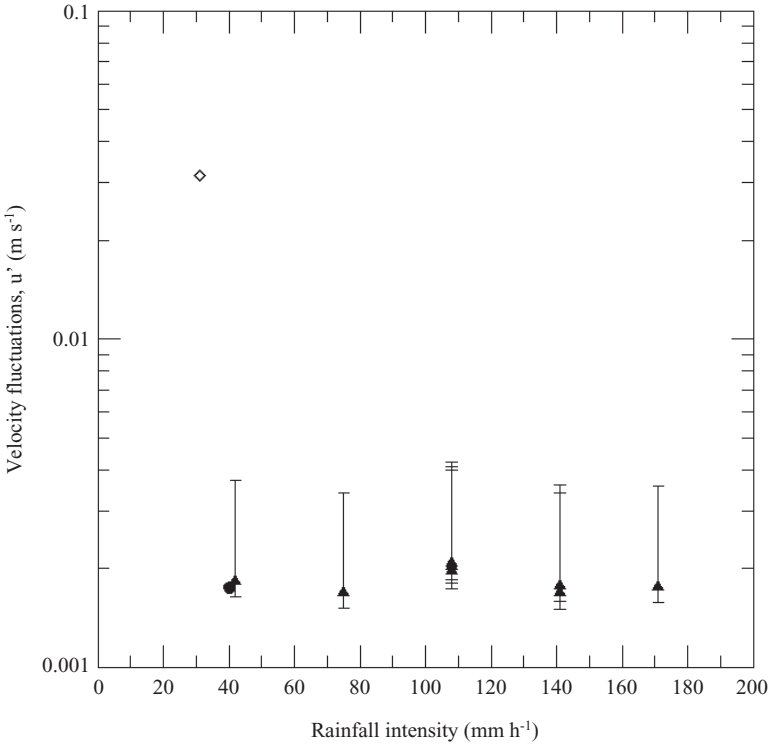

Figure 4 Velocity fluctuations recorded at constant depth of 31mm showing relative invariance to rainfall intensity. Triangles, *u'* present study; circle *w'* (Braun 2003) (interpolated); Hollow diamond, *u'* (Zappa *et al*. 2009) estimated as for Figure 3. Error bars represent the maximum uncertainty. The high limit corresponds to the raw *u'* value without filtering and noise deduction. The low limit corresponds to an estimate of a 10% error in the estimate of the noise level and frequency band in the calculation of *u'* through spectral partitioning.

on a static structure with a system that allowed the head to move vertically but with the ADV measurement volume projecting away from its body and any supporting appurtenances. It was important to ensure that the turbulence measurements were taken beneath a sufficiently clear area freely irradiated with rain droplets.

The selected geometric arrangement was judged to be the least intrusive and the selection was justified by subsequent analysis of the captured data.

The water column was seeded with 10-30μm diameter white pliolite and rendering clay which was then mixed over the entire depth at least 5 minutes before any recording of data. The seeding maintained an acoustic signal to noise ratio greater than 15 during the measurement period and the time delay before

recording was to allow turbulence generated by the stirring to be dissipated. Testing showed that 5 minutes was an adequate delay to ensure that measurements were not contaminated by the initial seeding process. An ADV beam check was also carried out before each measurement.

Preliminary static measurements showed that the turbulent velocities generated by the rainfall were very small. Consequently, for static measurements the ADV velocity range was set at its most sensitive level of ± 30mm s^{-1}. Measurement ensembles consisting of 163.84 s of 25Hz velocity samples were used to characterise the turbulence over a depth range between 0.031m and 0.151 m. Studies by Voulgaris and Trowbridge (1998) have shown that accurate measurement of turbulence properties can be obtained from ADVs provided that the geometric nature of the instrument and the underlying acoustic noise is properly recognised. The practical outcome of this is that the root mean square noise levels are approximately 5 times greater for those velocity components measured parallel to the ADV head (v' and w' in this present study, Figure 1) in comparison to that of the head-normal component (u'). Voulgaris and Trowbridge (1998) showed that the ADV reliably measures the u' component directly provided that the turbulence levels are not too high.

Representative velocity spectra obtained from the static ADV measurements are shown in Figure 2. Following Voulgaris and Trowbridge (1998) and Nikora and Goring (1998), the ambient acoustic noise was determined directly from the measured velocity spectra. In Figure 2, the instrument acoustic noise level is clearly apparent above 45rad s^{-1}. The spectra shown in Figure 2 also show low frequency (<8rad s^{-1}) velocity fluctuations induced by seiches and other low frequency motions within the tank itself. The intensities of velocity fluctuations directly induced by the rain were calculated by partitioning the spectra at the minimum spectral level at the lower frequencies and then deducting the acoustic noise from the remaining high frequency spectrum. This process assumes that the instrument noise is uncorrelated to the velocity fluctuations (Bradshaw 1971).

Figure 3 shows the assembled fluctuating velocity profiles obtained from these measurements. It can be observed that the rms magnitudes of the v' and w' remain approximately 40% higher than the comparable u' values as might be anticipated from Figure 2.

Given the small differences observed between the LR and HR we carried out additional turbulence measurements near the surface for a broader range of rainfall intensities. This was achieved by modifying the settings of the rainfall simulator given by Shelton *et al.* (1985) to obtain near uniform rainfall. Figure 4 shows the velocity fluctuations at 31mm depth as a function of the rainfall intensity. These measurements confirm the weak dependence between the intensity of the velocity fluctuations and the rainfall rate. Observations from Braun (2003) are included in

Figure 4 as a comparison.

4. Turbulence spectra

Measurements of turbulent dissipation rates are conventionally obtained by fitting the Kolmogorov model of the inertial sub-range of the wave number spectrum (under the assumption of isotropic turbulence). The inertial sub-range is given by:

$$\Phi_k = K' \varepsilon^{2/3} k^{-5/3} \tag{1}$$

where Φ_k = wave number spectra of the velocity fluctuations, K' a constant depending on the velocity component (Tennekes and Lumley, 1974, p. 273),

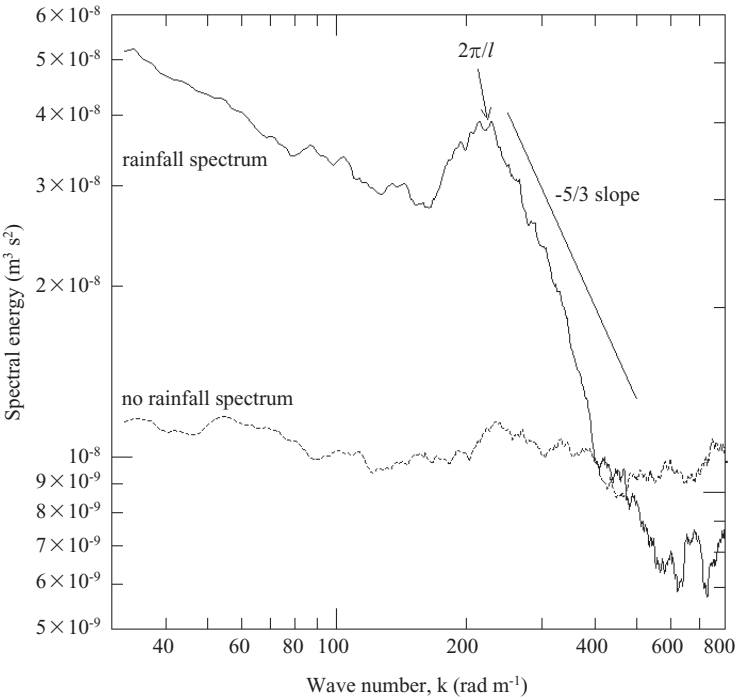

Figure 5 Representative wave number spectra obtained from the towing trolley experiments for the *w'* velocity component (ADV mounted focusing at 0.037m depth). Plotted spectra are the mean of 4 independent measurements, smoothed with 11 point bin averages. Dashed line shows the spectrum obtained in the absence of rainfall and shows little modulation with wave number. Solid line shows the high rainfall case. A line with −5/3 slope is shown as a reference. The integral turbulence length *(l)* for the high rainfall case is indicated. Note the higher noise levels in comparison with the static measurements shown in Figure 2.

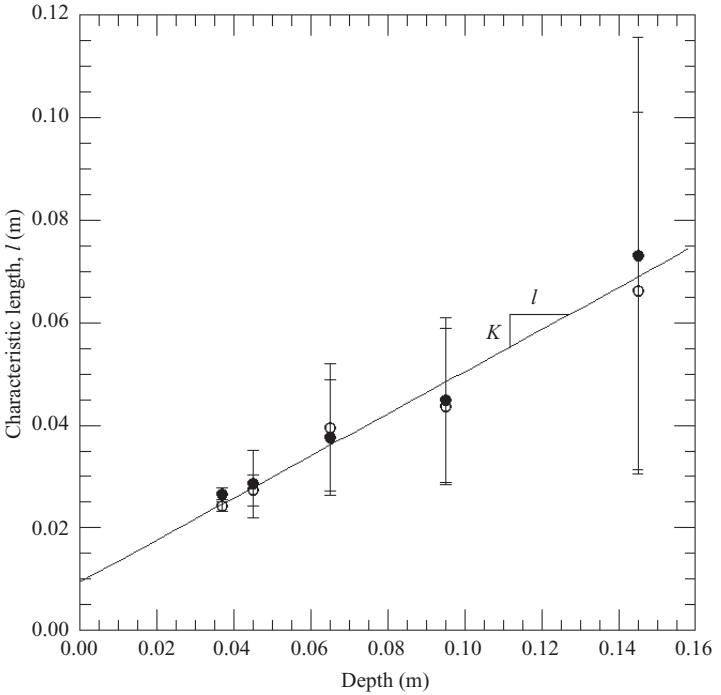

Figure 6 Vertical profile of the turbulent integral length scale *(l)* obtained from the intensity spectra (ADV mounted on a moving trolley measurements). The dashed line shows a linear fit with a slope equivalent to the Von Karman parameter, $\kappa = 0.41$.

ε = turbulent kinetic energy dissipation rate per unit volume and k = characteristic eddy wave number.

An attempt to measure the dissipation via this method involved profiling with the ADV along the still water tank at speed $U_{profile}$ and invoking Taylor's frozen turbulence hypothesis (where $U_{profile} \gg u'$, Tennekes and Lumley, 1974, p. 253). A mean speed of $U_{profile} = 0.085 m\ s^{-1}$ was used with the ADV measurement volume projected forward of the trolley assembly.

For each measurement case, smoothed spectra were obtained by averaging four repeat measurements. The corresponding wave number spectrum in the presence of rainfall (with acoustic noise deducted) yielded an energy peak at the integral turbulence length l and a form of energy spectrum compatible with determining a dissipation rate.

In spite of our efforts we considered that the estimates of the dissipation rate were unsatisfactory due to the increased noise inherent in the measurements caused by: 1) The increase in the ADV velocity range to $\pm 300 mm\ s^{-1}$ thereby also

increasing the system acoustic noise, 2) Contamination of the measurements in the *u'* direction caused by the along-tank jitter in the instrument package motion in spite of considerable care in the manufacture and operation of the trolley system.

Despite the lack of success in quantifying the dissipation rates, we observed that the integral turbulence length scale given by the peak of the spectrum was not severely affected by the noise. Figure 6 shows the wave number spectra of the *w'* component from which the integral turbulence length (l) can be obtained. This component was selected because it exhibited the lowest noise level and approximately a white spectral response in the absence of rainfall (Figure 5). The error in l was estimated from the upper and lower wave number values of the peak of the spectrum.

Craig and Banner (1994) proposed a turbulence diffusion model for wind and white-capping induced surface turbulence in the ocean that can be applied in absence of mean shear. To our knowledge this is the best existing model to describe and quantify the turbulence profile in the surface boundary layer of the ocean. This model uses a "law of the wall" type of expression for the integral length shown in equation (2). In the case of rainfall there is no shear induced by wind, breaking or a solid boundary. However the drop impact process must produce sufficient vorticity capable of creating turbulence at the surface. Since there is no advection, turbulence is diffused down in the water column in a similar mechanism to that in the Craig and Banner (1994) model.

The depth profile l is presented in Figure 6 according to the expression adopted by Craig and Banner (1994) for their ocean surface turbulence diffusion model (see their p.2546):

$$l=\kappa(|z|+z_0) \tag{2}$$

where $\kappa=0.41$ is the Von Karman parameter, z is the vertical coordinate and z_0 is the roughness length.

A value of $z_0=0.023$ can be obtained by fitting eq. (2) to the data in Figure 6 by minimising the mean squared error.

5. Comparison with Zappa *et al.* (2009)

Zappa *et al*. (2009) carried out turbulence measurements under rainfall using two types of acoustic instruments: a coherent Doppler sonar and a modular acoustic sensor. Estimates of the dissipation rate were carried out fitting a Kolmogorov type of spectrum as in eq. (1), assuming an advection velocity equal to the mean measured flow. Mean rainfall rates between 35 and 75 mm h^{-1} (according to their bucket measurements) were generated with nozzles located 10m above the water surface.

In contrast to our measurements, they reported very high turbulent dissipation rates of O(10^{-2} m^2 s^{-3}) which are normally observed in highly turbulent flows such as under breaking waves and hydraulic jumps (e.g. Thorpe 2005, p.25). However they found a weak dependence of the dissipation as a function of the rainfall intensity (their Figure 9) which agrees with the observations of this study.

Zappa *et al*. (2009) also found that the gas transfer rate at the air-water interface depends on the amount of turbulence dissipation induced by rainfall kinetic energy flux (*KEF*) supporting the work of Ho *et al*. (2000). Conversely laboratory experiments by Takagaki and Komori (2007) showed poor correlation between the air-water gas transfer rate and the rainfall *KEF*.

Figure 3 and Figure 4 show velocity fluctuations estimated from their dissipation measurements obtained using eq. (2) with the value of z_0 obtained in this study and the scaling relationship given in eq. (3) assuming $A=1$.

$$\varepsilon = A\frac{u'^3}{l} \tag{3}$$

where ε is the turbulent kinetic energy dissipation rate per unit volume and A is a constant O(1), (Craig and Banner 1994), (Tennekes and Lumley, p.20).

6. Vertical energy fluxes

The rainfall *KEF* can be calculated using eq. (4) and the drop sizes distribution and drop impact velocities given in Shelton *et al*. (1985). The calculated *KEF* for LR and HR are 0.85 and 1.11 watt/m^2 respectively.

$$KEF = \frac{1}{2}\int_0^\infty \rho \cdot I \cdot f(\phi) \cdot V_{\text{drop}}^2(\phi) d\phi \tag{4}$$

where *KEF* is the rain energy flux, I = rainfall intensity, ϕ rain drop diameter, $f(\phi)$ = rain drop diameter probability distribution, $V_{drop}(\phi)$ = raindrop impact velocity as a function of ϕ.

In contrast, the energy flux dissipated due to sub-surface turbulence can be estimated in 0.002 watt/m^2 by integrating the dissipation in eq. (3) from the bottom of the tank to z_0. For this calculation the *u'* profile in Figure 3 was extrapolated following (Craig and Banner 1994, eq. 25). The velocity fluctuations profile, $u' = 1.58x10^{-6}\ (|z|+z_0)^{-2.4}$ was obtained by least squares fitting. The turbulent dissipation energy flux is approximately 0.2% of the *KEF* indicating very high dissipation levels at the surface layer. This finding is in contrast with conclusions of Le Mehaute and Khangaonkar (1990).

7. Conclusions and Recommendations

An experimental investigation of subsurface turbulence generated by simulated rainfall has been completed.

Measuring low levels of turbulence using acoustic instruments has specific challenges. The spectral separation method used in this study showed that the near surface fluctuations are isotropic and that the head normal and head parallel velocity measurements can be reconciled. Adequate seeding, beam checks, velocity settings and data processing considering the noise and long fluctuations are fundamental to obtain reliable estimates of the turbulence statistics from acoustic instruments.

The results of this study showed that the energy transfer between rainfall and subsurface turbulence is a weak process and that the subsurface velocity intensities are comparatively weak.

This is in agreement with the work of Braun (2003) but contrary to the conclusions of a recent study by Zappa *et al*. (2009). Furthermore, measurements showed that subsurface turbulence is weakly dependent on rainfall intensity (i.e. *KEF*). This is, although, in agreement with Zappa *et al*. (2009). The rest of the energy is probably dissipated very near the air-water interface where the interaction of capillary ripples and turbulence, drop splashes, air entrainment and other complex processes take place.

The following aspects of the Craig and Banner (1994) pure turbulence diffusion model can be contrasted to our measurements:

1) Measured integral turbulence lengths agree with their "law of the wall" turbulence length model, see their eq. 1.
2) z_0 obtained in this study is consistent with the O(10mm) drop penetration observations by Braun (2003) and our own visualizations.
3) Measured velocity fluctuations profile decays faster (proportionally to $(|z|+z_0)^{-2.4}$ as compared to $(|z|+z_0)^{-0.8}$, see their eq. 25), probably due to viscous dissipation being significant in flows with low levels of turbulence, (Pope 2000, p.235)

Observed differences with Craig and Banner (1994) may be anticipated given that their model assumed strong turbulence.

Future research is recommended to quantify energy fluxes in the first millimeters of the air-water interfaces under rainfall conditions. It is likely that viscous processes may have more significance than previously anticipated. A re-analysis of valuable turbulence measurements under rainfall carried out by Zappa *et al*. (2009) considering some of the data processing techniques used in this study may reconcile observations in both studies.

References

Bradshaw P. (1971), An introduction to Turbulence and its Measurement (Book), Pergamon Press, First edition.

Bliven L., Sobieski P. and Craeye C. (1997), Rain generated ring-waves: measurements and modelling for remote sensing (Journal), *Int. J. Remote Sensing, Vol. 18*, No. 1, 221-228.

Braun N. (2003), Untersuchungen zur Radar-Rückstreuung und Wellendämpfung beregneter Wasseroberflächen, Dissertation, Universität Hamburg, Fachbereich Geowissenschaften, "On the Radar Backscattering and Wave Damping on Water Surfaces Agitated by Rain" (PhD. Thesis Dissertation).

Craeye, C., and P. Schlussel (1998), Rainfall on the sea: Surface renewals and wave damping (Journal), *Boundary Layer Meteorology, 89,* 349 – 355, doi: 10. 1023/A: 1001796911059.

Craig P. and Banner M. (1994), Modelling wave-enhanced turbulence in the ocean surface layer (Journal), *J. Phys. Oceanogr.*, 24, 2546–2559.

Ho, D. T., W. E. Asher, L. F. Bliven, P. Schlosser, and E. L. Gordan (2000), On the mechanisms of rain-induced air-water gas exchange (Journal), *J. Geophys .Res., 105 (C10),* 24, 045–24, 057, doi:10.1029/1999JC00028.

Houk D. and Green T. (1976), A note on surface waves due to rain (Journal), *J. Geophys . Res. 81*, 4482.

Kawamura, H. and Toba, Y. (1988) Ordered motion in the turbulent boundary layer over wind waves. *J. Fluid Mech.*, **197**: 105-138

Le Méhauté B. and Khangaonkar T. (1990), Dynamic interaction of intense rain with water waves (Journal), *J. Phys. Oceanogr.,* Vol 20, pp. 1805-1812.

Manton, M. J. (1973), On the attenuation of sea waves by rain (Journal), *Geophys. Fluid Dyn., 5*, 249-260.

Nikora, V. and Goring D. (1998), ADV Measurements of Turbulence: Can We improve Their Interpretation? (Journal), *J. Hydr. Engrg. Volume 124*, Issue 6, pp. 630-634 (June 1998), ASCE.

Nystuen J. (1990), A note on the attenuation of surface gravity waves by rainfall (Journal), *J. Geophys. Res. Vol 95*, pp. 18353-18355.

Pope S. (2000), Turbulent flows (Book), Cambridge University Press.

Poon Y., Tang S. and Wu J (1992), Interactions Between Rain and Wind Waves (Journal), *J. Phys. Oceanogr.*, *Vol 22*, pp. 976-987.

Rapp, R. J. and W. K. Melville (1990), Laboratory measurements of deep water breaking waves (Journal), *Phil. Trans. R. Soc. A, 331*, pp. 735–800.

Shelton C. H., von Bernuth R. D., Rajbhandari S. P. (1985), A Continuous Application Rainfall Simulator (Journal), *American Society of Agricultural Engineers*, Vol 28(4), Paper N 84-2049.

Takagaki N. and Komori S. (2007), Effects of rainfall on mass transfer across the air-water interface (Journal), *J. Geophys. Res., 112,* C06006, doi:10.1029/2006JC003752.

Thorpe S.A. (2005), The Turbulent Ocean (Book), Cambridge University Press.

Tsimplis M.N. (1992), The effect of Rain in calming the Sea (Journal), *J. Phys. Oceanogr.*, *Vol 22*, pp. 411.

Tennekes H., Lumley J. L. (1974), A First course in Turbulence (Book), 15th printing MIT Press Design Department.

Voulgaris G. and Trowbridge J. (1998), Evaluation of the acoustic Doppler velocitmeter (ADV) for Turbulence Measurements (Journal). *J. Atmospheric and Ocean Technology,*

15, 272-289, American Meteorological Society.

Zappa, C. J., D. T. Ho, W. R. McGillis, M. L. Banner, J. W. H. Dacey, L. F. Bliven, B. Ma, and J. Nystuen (2009), Rain-induced turbulence and air-sea gas transfer (Journal), *J. Geophys. Res., 114*, C07009, doi:10.1029/2008JC005008